Effect of Gold Nanoparticles on Prostate Dose Distribution under Ir-192 Internal and 18 MV External Radiotherapy Procedures Using Gel Dosimetry and Monte Carlo Method

Khosravi H.[1], Hashemi B.[2]*, Mahdavi S. R.[3], Hejazi P.[4]

[1]Ph.D. Candidate, Department of Medical Physics, Tarbiat Modares University, Tehran, Iran
[2]Associate Professor, Department of Medical Physics, Tarbiat Modares University, Tehran, Iran
[3]Assistant Professor, Department of Medical Physics, Iran University of Medical Sciences, Tehran, Iran
[4]Assistant Professor, Department of Medical Physics, Semnan University of Medical Sciences, Semnan, Iran

ABSTRACT

Background: Gel polymers are considered as new dosimeters for determining radiotherapy dose distribution in three dimensions.

Objective: The ability of a new formulation of MAGIC-f polymer gel was assessed by experimental measurement and Monte Carlo (MC) method for studying the effect of gold nanoparticles (GNPs) in prostate dose distributions under the internal Ir-192 and external 18MV radiotherapy practices.

Method: A Plexiglas phantom was made representing human pelvis. The GNP shaving 15 nm in diameter and 0.1 mM concentration were synthesized using chemical reduction method. Then, a new formulation of MAGIC-f gel was synthesized. The fabricated gel was poured in the tubes located at the prostate (with and without the GNPs) and bladder locations of the phantom. The phantom was irradiated to an Ir-192 source and 18 MV beam of a Varian linac separately based on common radiotherapy procedures used for prostate cancer. After 24 hours, the irradiated gels were read using a Siemens 1.5 Tesla MRI scanner. The absolute doses at the reference points and isodose curves resulted from the experimental measurement of the gels and MC simulations following the internal and external radiotherapy practices were compared.

Results: The mean absorbed doses measured with the gel in the presence of the GNPs in prostate were 15% and 8 % higher than the corresponding values without the GNPs under the internal and external radiation therapies, respectively. MC simulations also indicated a dose increase of 14 % and 7 % due to presence of the GNPs, for the same experimental internal and external radiotherapy practices, respectively.

Conclusion: There was a good agreement between the dose enhancement factors (DEFs) estimated with MC simulations and experiment gel measurements due to the GNPs. The results indicated that the polymer gel dosimetry method as developed and used in this study, can be recommended as a reliable method for investigating the DEF of GNPs in internal and external radiotherapy practices.

Keywords

Brachytherapy, Ir-192, MAGIC-f Polymer Gel Dosimeters, Monte Carlo Method, Nanoparticles, Prostate, Radiotherapy

*Corresponding author:
B. Hashemi
Department of Medical Physics, Tarbiat Modares University, Al-Ahmad and Chamran Crossroads, Tehran, Iran
E-mail: bhashemi@modares.ac.ir

Introduction

Over the recent years, the effect of GNPs in common radiotherapy practices has been studied extensively by using experimental measurements and MC simulations. Although the idea of increasing the dose by using some elements with high atomic

numbers has been proposed several decades ago, following the invention and compatibility of GNPs with biological systems, scientists have stimulated to investigate further applications of such elements in radiotherapy practices. The results of most of the studies in this field have confirmed an increase of the radiation absorbed doses to various tumors in the presence of GNPs. However, the results are still controversial regarding the involved and prominent interaction processes of ionizing radiation with the GNPs resulted in tumor DEFs. The most effective parameters affecting the higher doses investigated by using experimental dosimetry and MC methods include: the dimension of nanoparticles, high molar concentrations, and lower energies of the photons or gamma rays used in various studies [1-14].

If the energy of the photon is greater than 1.02 MeV, the pair production reaction will occur and result in the electron and positron production. Up to 5 MeV of energy, the Compton scattering is noticeable. However, above 5 MeV, the pair production interaction with high atomic number elements becomes dominant. Apart from the Compton scattering, the cross section of the photon with different materials depends highly on their effective atomic number for the photoelectric (Z4) and pair production (Z2.4) interactions [15-16]. Therefore, due to the dominance of the pair production interaction with GNP atoms, it is expected that a considerable amount of energy is transferred to these nanoparticles. Consequently, the relevant DEF resulted from the presence of GNPs should be proportional to the ratio of the mass absorption coefficient (μ_{en}/ρ) of these nanoparticles to the water as a soft tissue equivalent material. The DEFs for the beams with different spectrums are expressed by the following equation [17]:

$$DEF = 1 + \frac{k_{NP}\int_{E=0}^{E_{max}} \psi(E)\left(\frac{\mu_{en}}{\rho}\right)_{NP,E} dE}{\int_{E=0}^{E_{max}} \psi'(E)\left(\frac{\mu_{en}}{\rho}\right)_{water,E} dE}$$

where NP, μ_{en}/ρ, k_{NP}, and E represent the "nanoparticles", "mass energy absorption coefficient", "weighting percentage of the nanoparticles in the mixture", and "radiation beam energy", respectively.

Various conventional dosimeters such as ion chambers, TLDs and diodes can measure only the point doses under limited conditions. The film dosimetry can also specify two dimensional dose distributions. Various dosimetry methods are often used to confirm radiotherapy precisions. In brachytherapy, especially for evaluating the complex dose distributions resulted from interstitial practices, it is impossible to use such conventional dosimetry methods. Because of high dose gradients in such practices, a large number of point dosimeters with very small sizes are needed to be placed around the radiation sources. In addition, the dose values are highly dependent on the location and small movements of such dosimeters leading to high levels of dosimetric errors. Moreover, some of the conventional dosimeters are not tissue-equivalent and their presence causes the distortion of radiation geometries specified later in dose distributions. Even by using the film dosimeters, radiation dose distributions can be measured only in a two-dimensional surface. These restrictions have raised particular attention of researchers to use various gel polymers for measuring complex dose distributions in radiotherapy practices [18-19].

The MAGIC-f gel, as an appropriate three-dimensional and tissue-equivalent dosimeter, has been successfully used to determine quantitatively the DEFs resulted from the presence of GNPs as a compatible radio-sensitizer in various target organs. This gel can be used potentially to assess the effects of using GNPs in

radiotherapy practices [20]. Recently, a polyacrylamide gel (nPAG) has also been used to measure the increase of the absorbed dose rate in the presence of GNPs in different energy ranges [21]. Overall, the gel dosimetry is reported as an appropriate tool for accurate dosimetric measurement when the nanoparticles are used in radiotherapy practices especially at kV energies.

In this study, the effect of GNPs on the DEFs in prostate and bladder under conventional radiotherapy practices, a kV internal brachytherapy (Ir-192 sources) and high MV external beam (18 MV energy of a Varian linac), has been investigated experimentally by using a new formulation of the MAGIC-f gel dosimeter as well as by MC simulations done by the MCNPX code.

Material And Methods

Design and Construction of Pelvic Phantom

The constructed Plexiglas pelvic phantom has an elliptical shape with an overall dimension of 200×200×300 mm^3 in which the positions of the human bladder, prostate, rectum and bone tissue are defined. The bladder, prostate, and rectum incorporated in the phantom have a hollow cylindrical form wherein the desired gel can be poured. It should be noted that two different caps were constructed for the prostate. The cap designed for the internal radiotherapy practices has appropriate holes to accommodate and hold the brachytherapy needle sources, while the cap designed for external radiotherapy has no hole. The phantom was designed and constructed according to the model made by CIRS Company (Model 002PRA, Computerized Imaging Reference Systems, USA). Figure 1 shows a view of the constructed pelvic phantom.

To obtain the gel dosimeter calibration curve, small plastic falcon tubes with a 20 mm outer diameter, 100 mm height, and 17 ml volume were used.

Figure 1: A View of Constructed Pelvic Phantom

Gold Nanoparticle Synthesis

GNPs were produced using gold salt and chemical reduction method as proposed by Kupiec et al. [22]. The GNPs were synthesized with appropriate amounts of its components to have a diameter of 15 nm. The average size of our GNPs products was proved by using the DLS (Dynamic Light Scattering, Malvern, UK) and TEM (Transmission Electron Microscopy) tests.

Incorporating GNPs in the Gel

After fabricating 500 ml of MAGIC-f gel, based on its original constituents [23], although with a new formulation, it was divided into two separate volumes of 100 and 400 ml. Then, the 100 ml volume of the gel was transferred to another container wherein the GNPs solution was added to reach a 0.1 mM concentration of the GNPs in the final gel mixture. The gel mixture was stirred for a period of 5 minutes. Thereafter, the gel was poured in the calibration tubes as well as the prostate (with or without the presence of GNPs), bladder, and rectum containers of

the pelvic phantom and kept in a refrigerator at 4°C.

Treatment Planning and Irradiation

CT-Scan images are required for radiotherapy treatment planning. Therefore, the CT scan of the pelvic phantom was performed using a Siemens (Germany) scanner. The required treatment planning was performed for both internal and external radiotherapy procedures.

For the external radiotherapy, at first, the size, direction, and any other information related to the pelvic phantom dimensions were calibrated against its image. Then, by considering the size and location of the prostate in the phantom, four orthogonal radiation fields were defined for treating prostate by using Core PLAN software (Seoul C&J, South Korea). The treatment planning specifications are provided in figure 2 and table 1.

For internal brachytherapy practice, the required dose is selected from the planning target volume (PTV) defined by the oncologist. Flexiplan software (ELECTA, Sweden) was used for our brachytherapy treatment planning to compute the location of the source (Dwell-position) and the amount of the time at each stop location (Dwell-time)

Table 1: Treatment Planning Specifications Used for 18 MV External Radiotherapy of Pelvic Phantom by Varian 2100 linac

Energy	18 MV
Number of fields	4
Distance of the source to the center of the prostate	100 cm
Field size	6 cm×6 cm
Delivered Dose	200 cGy
Monitor Unit/Fraction	204.9

for this procedure. In the treatment planning done for this radiotherapy procedure, isodose curves can be seen on all of the images and CT slices. Two different views of the isodose curves obtained for this procedure can be observed in figure 3.

Prior to implementing internal and external radiotherapy planning as described above and to calibrate our fabricated MAGIC-f gel, the tubes containing the gel were irradiated to different levels of known doses measured with a calibrated dosimeter provided by the Varian linac. After calibrating MAGIC-f gel, the phantom was irradiated to the high dose rate internal brachytherapy and the 18 MV external radiotherapy beams provided by the Ir-192 sources and Varian linac separately at all radiotherapy stages.

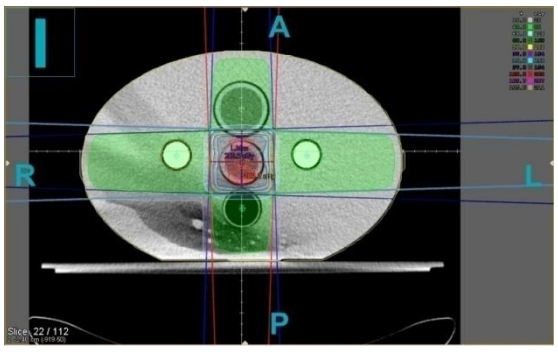

Figure 2: Treatment planning Performed on Pelvic Phantom under 18 MV External Radiotherapy Procedure by Varian 2100 linac

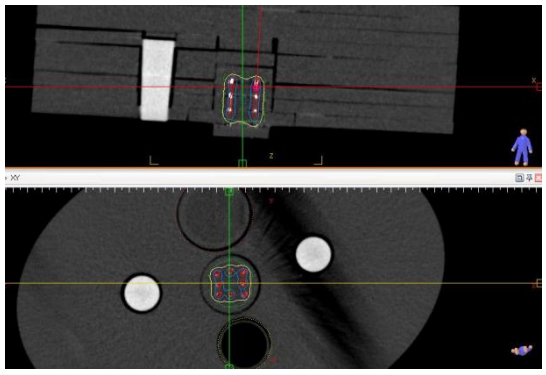

Figure 3: Treatment Planning Performed on Pelvic Phantom under Internal Brachytherapy Procedure by Ir-192 Sources

MRI Reading and Processing

At 24-hour post of the irradiation procedures, the gels were read using a 1.5 Tesla Siemens MRI scanner (Germany). It should be reminded that prior to the imaging process, the phantom and calibration tubes were taken to an isothermal room and kept there for a period of 4 hours. MRI imaging process was performed according to the protocol given in table 2.

Table 2: Protocol Used for Reading MRI Images of Pelvic Phantom and Calibration Gel Tubes.

Parameter	Value
Field of view (mm)	300
Dimensions of the matrix	256×256
Slice thickness (mm)	4
Time of echo (ms)	22
Pulse repetition time (ms)	3000
Pixel dimensions(mm2)	0.9×0.9
Number of Echo	16

The matrices plotted from MRI R2 signals for each section were calculated by MATLAB software. The absolute doses and relative dose distribution curves were extracted from R2 signals of the MRI images.

Monte Carlo Simulation

MCNPX code was used for MC calculation. After validating linac structures and its 18 MV photon beam parameters and also the Ir-192 sources (based on TG-43 protocol [24]), the pelvic phantom was simulated according to its actual dimensions. In general, five materials were simulated in the pelvic phantom including: MAGIC-f gel, GNPs, Teflon (representing femur bone) air (representing rectum) and Plexiglas (representing soft tissues of the rest of the pelvic phantom).

The simulated phantom was irradiated based on the same conditions and protocols as used in the internal and external experimental treatment planning procedures.

Results

The results will be presented from both our experimental measurements and MC calculations for both of internal and external radiotherapy procedures performed in this study as described in the previous section. At experimental stage, the calibration process of the gel resulted in a linear relationship between MRI R2 values and the doses received by the calibration gel tubes (figure 4).

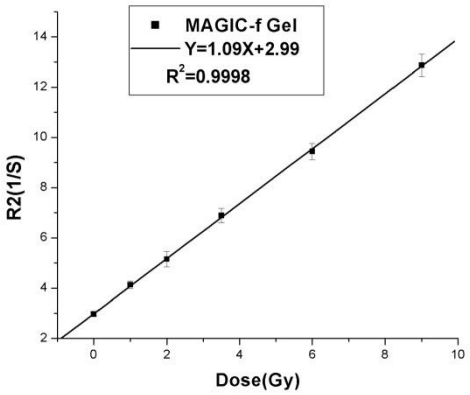

Figure 4: MAGIC-f Gel Calibration Curve Determined from Experimental Measurement

The isodose curves of the bladder and prostate (with and without the presence of GNPs) which were measured experimentally and calculated by MC simulations in the pelvic phantom in two different slices, located at A) X=+ 0.4 cm and B) X=0 cm, for the external radiotherapy procedure are presented in figure 5.

The isodose curves of the bladder and prostate (with and without the presence of GNPs) which were measured experimentally and calculated by MC simulations in the pelvic phantom in two different slices, located at A) X=+0.4 cm and B) X=0 cm,

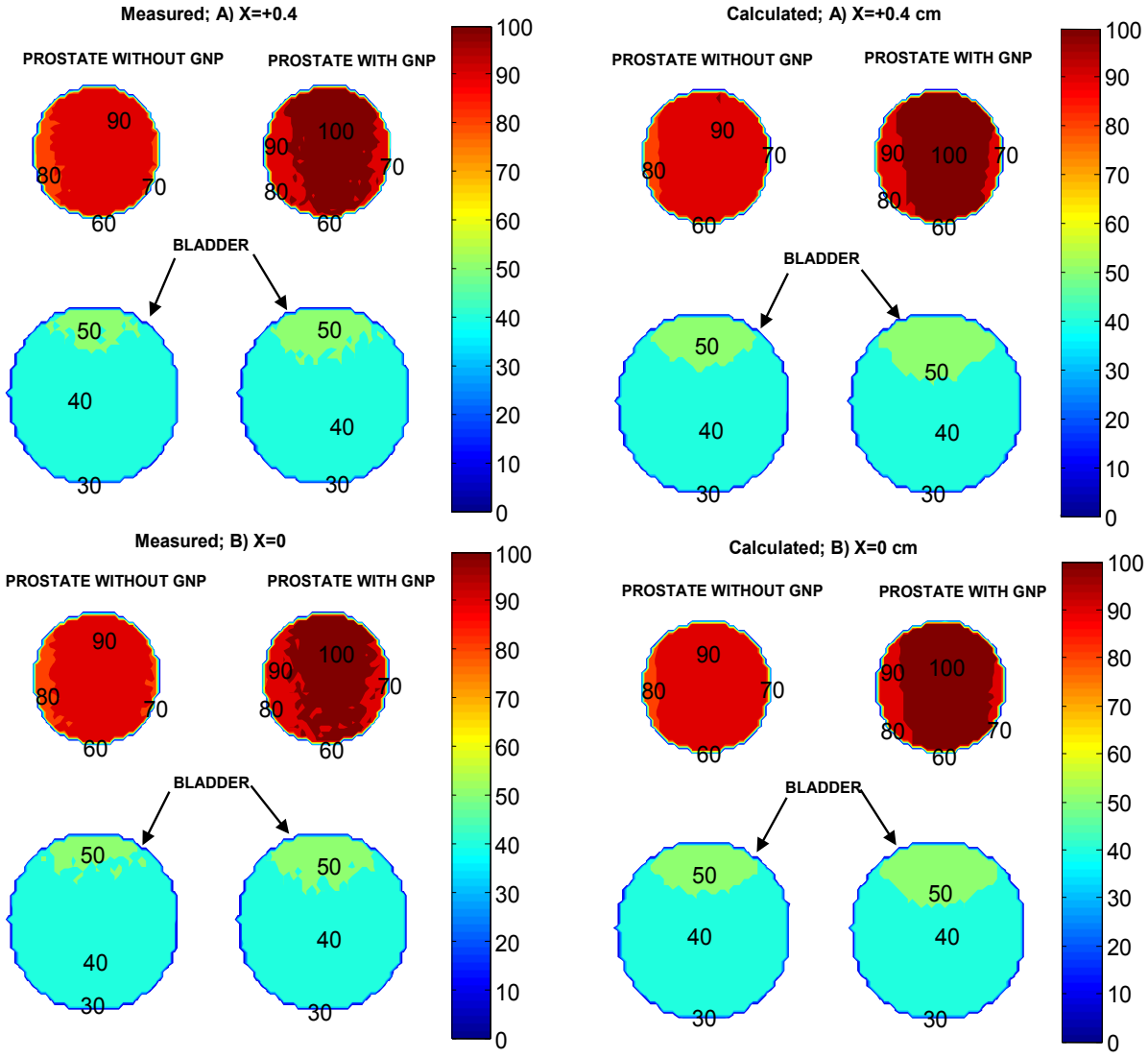

Figure 5: Comparison of Isodose Curves Measured Experimentally with Gel and Calculated by MC Calculations at two Different Slices for18 MV (Varian linac) External Radiotherapy Procedure

for the internal radiotherapy procedure are presented in figure 6.

The DEFs measured with the gel and calculated with MC method at two different slices of the pelvic phantom for the external radiotherapy procedure are presented in figure 7. At any region of interest, DEFs were derived by dividing the relative amount of the doses at any pixel of the images measured/calculated with the presence of the GNPs.

The mean values of the DEFs estimated from the experimental measurements and simulated calculations for prostate from 18 MV external radiotherapy procedures at two different slices of the pelvic phantom are shown in table 3.

The mean values of the DEFs measured experimentally with the gel and calculated with MC simulations at the two different slices of the pelvic phantom from internal

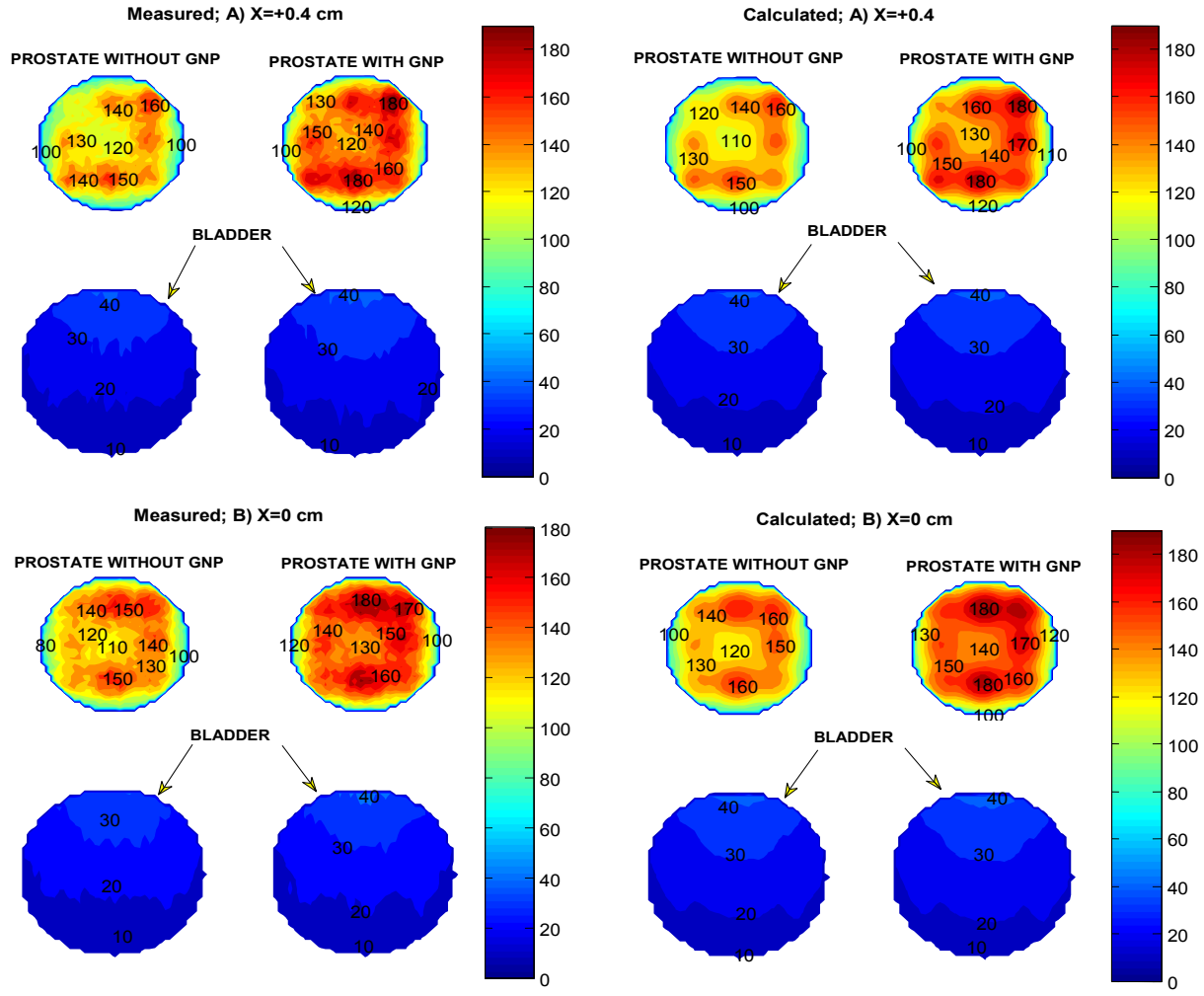

Figure 6: Comparison of Isodose Curves Measured Experimentally with Gel and Calculated by MC Calculations at two Different Slices for Internal Brachytherapy (Ir-192) Procedure

Table 3: Mean Values of DEFs Measured Experimentally with Gels and Calculated by MC Simulations due to the Presence of GNPs in Prostate of the Pelvic Phantom from 18 MV (Varian linac) External Radiotherapy Procedure at Two Different Slices

Slice	X=+0.4 cm	X=0 cm	Total
DEF(Measured)	1.09± 0.02	1.08± 0.02	1.08± 0.01
DEF(Calculated)	1.078 ± 0.002	1.075 ± 0.002	1.075 ± 0.002

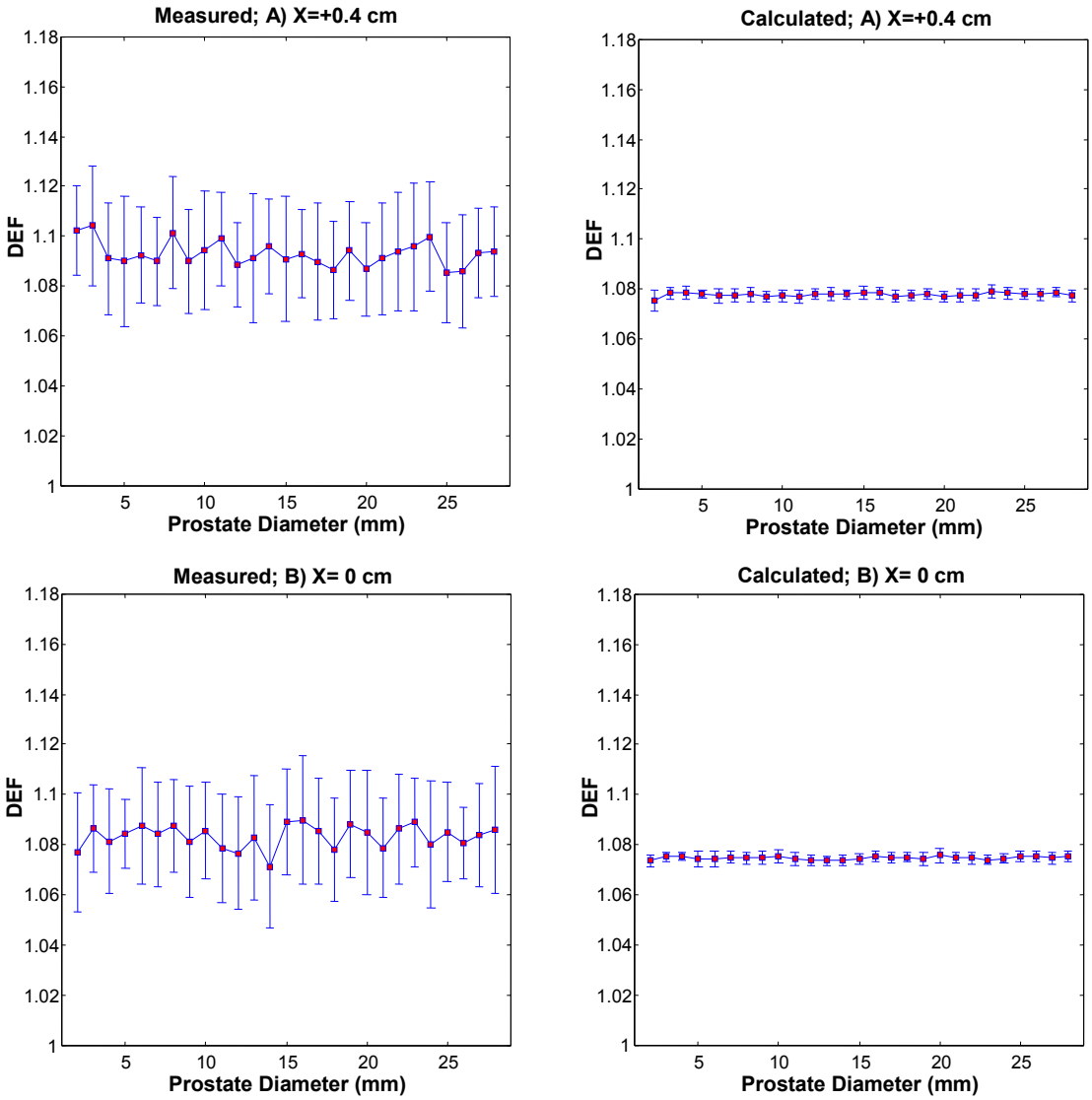

Figure 7: Experimental and Simulated DEFs Resulted from GNPs for Prostate in Pelvic Phantom from 18 MV (Varian linac) External Radiotherapy Procedure at two Different Slices (A: X=+0.4 cm, B: X=0 cm)

brachytherapy procedure (with Ir-192 sources) are presented in figure 8. These DEFs, at any region of interest, were also estimated by dividing the relative amount of the doses at any pixel of the images measured/calculated with the presence of the GNPs.

The mean values of the experimental and simulated DEFs for prostate from internal brachytherapy procedure at two different slices of the pelvic phantom are shown in table 4.

Discussion and Conclusion

In the experimental part of this study, some dosimetric specifications of the fabricated MAGIC-f gel dosimeter including its linearity and dose resolution were assessed. The fabricated gel showed a linear dose response in a range of 0-900 cGy with a considerable increase up to 50 percent indicating a sat-

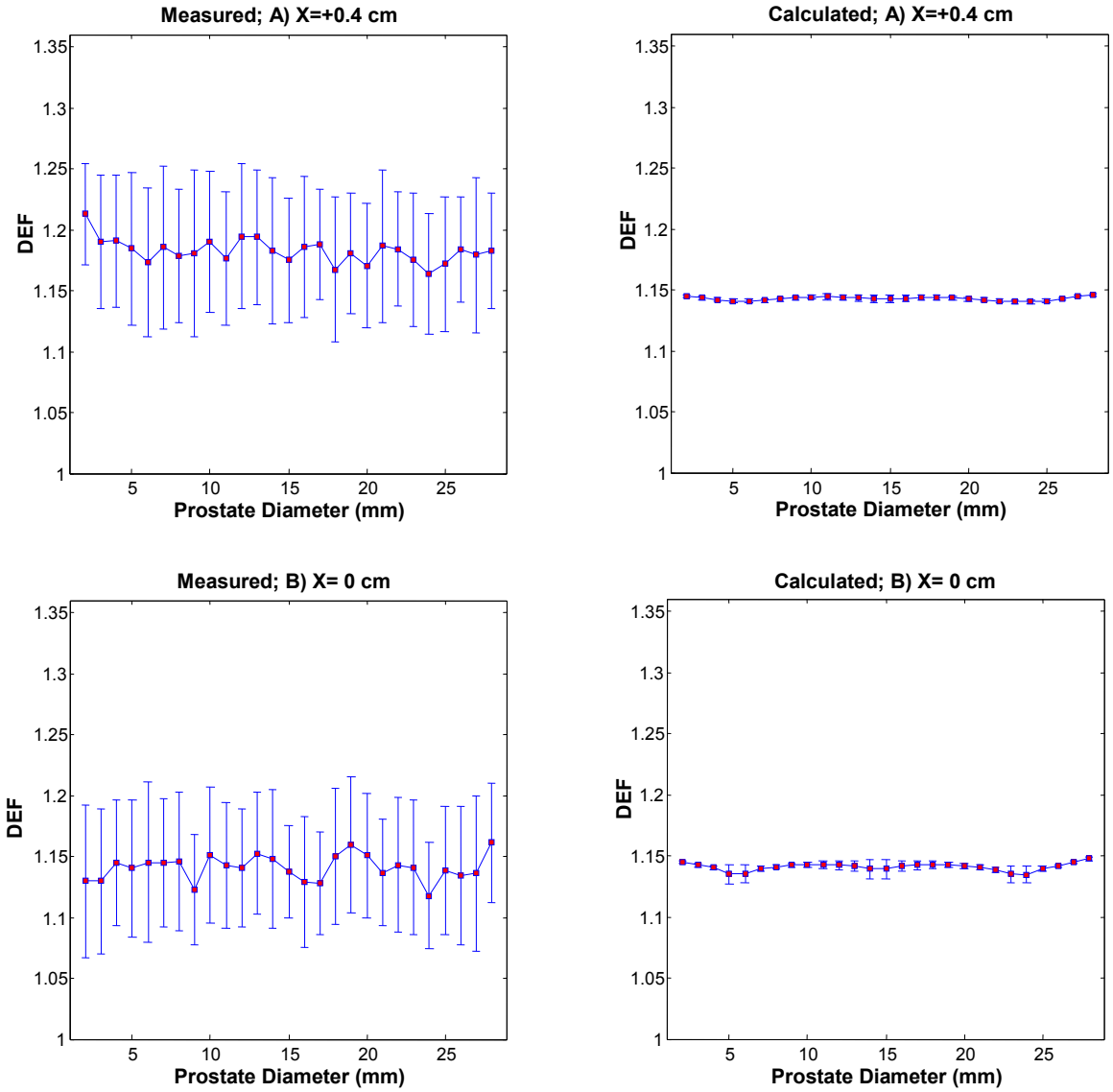

Figure 8: Experimental and Simulated DEFs Resulted from GNPs for Prostate in Pelvic Phantom from Internal Brachytherapy (Ir-192) Procedure at two Different Slices (A: X=+0.4 cm, B:X=0 cm)

Table 4: Mean Values of DEFs Measured Experimentally with Gels and Calculated by MC Simulations due to the Presence of GNPs in Prostate of the Pelvic Phantom from Internal Brachytherapy (Ir-192) Procedure at two Different Slices

Slice	X=+0.4 cm	X=0 cm	Total
DEF(Measured)	1.18± 0.06	1.14± 0.05	1.15± 0.03
DEF(Calculated)	1.143± 0.002	1.141± 0.005	1.141± 0.004

isfactory and well polymerization process. The dose response of the gel was also assessed with and without the presence of the GNPs for both internal and external radiotherapy modalities used commonly for prostate cancer treatment in a pelvic phantom. Our experimental results with gel dosimeter indicated a mean DEF of 9% (SD=1%) and 15% (SD=3%) due to the presence of the GNPs in prostate for external and internal radiotherapy procedures, respectively.

The MC method was also used to simulate our experimental measurements and calculate DEFs in prostate resulted from GNPs for the same common internal and external radiotherapy modalities as investigated with experimental gel dosimetry method. MC results showed a mean DEF of 8.3% (SD=0.2%) and 14.1% (SD= 0.4%) due to the presence of GNPs in prostate for external and internal radiotherapy procedures, respectively.

Both experimental measurements and MC calculations indicated higher DEFs in the target volume (prostate) for internal brachytherapy (Ir-192) of prostate in the presence of GNPs compared to those of high energy (18MV) external radiotherapy. This must have been mainly due to higher probabilities of the photoelectric effect in kV internal brachytherapy relative to MV external radiotherapy modality. Since, despite the increased probability of the pair production interaction at MV energies, the amount of the dose increase due to this interaction is less than that of the more dominant photoelectric interaction at kV energies [15, 16]. Furthermore, the ratios of the mass absorption coefficient (μ_{en}/ρ) of gold to water at low kVs is higher than those of the high MVs [17, 25].Therefore, it is expected that DEF in prostate in the presence of GNPs would be higher in internal low KV energy as used in brachytherapy compared to that of external MV energies as used in external radiotherapy modalities.

There was a good agreement between DEFs obtained by MC computational method and the experimental gel dosimetry measurements for GNPs concentration used in this study. The results demonstrate that fabricated MAGIC-f gel could be used as a suitable three-dimensional dosimeter for more extensive studies at various internal and external radiotherapy modalities and also with the presence of various concentrations of GNPs.

Conflict of Interest

None

References

1. Hainfeld JF, Slatkin DN, Smilowitz HM. The use of gold nanoparticles to enhance radiotherapy in mice. *Phys Med Biol*. 2004;**49**(18):N309-15. doi: 10.1016/j.nano.2014.05.006. PubMed PMID: 15509078.
2. Yih TC, Wei C. Nanomedicine in cancer treatment. *Nanomedicine*. 2005;**1**(2):191-2. doi: 10.1016/j.nano.2005.04.001. PubMed PMID: 17292078.
3. Kawasaki ES, Player A. Nanotechnology, nanomedicine, and the development of new, effective therapies for cancer. *Nanomedicine*. 2005;**1**(2):101-9. doi; 10.1016/j.nano.2005.03.002. PubMed PMID: 17292064.
4. Hirsch LR, Stafford RJ, Bankson JA, Sershen SR, Rivera B, Price RE, et al. Nanoshell-mediated near-infrared thermal therapy of tumors under magnetic resonance guidance. *Proc Natl Acad Sci U S A*. 2003;**100**(23):13549-54. doi: 10.1073/pnas.2232479100. PubMed PMID: 14597719; PubMed PMCID: PMC263851.
5. Loo C, Lowery A, Halas N, West J, Drezek R. Immunotargeted nanoshells for integrated cancer imaging and therapy. *Nano Lett*. 2005;**5**(4):709-11. doi: 10.1021/nl050127s. PubMed PMID: 15826113.
6. Chang MY, Shiau AL, Chen YH, Chang CJ, Chen HH, Wu CL. Increased apoptotic potential and dose-en-

hancing effect of gold nanoparticles in combination with single-dose clinical electron beams on tumor-bearing mice. *Cancer Sci*. 2008;**99**(7):1479-84. doi: 10.1111/j.1349-7006.2008.00827.x. PubMed PMID: 18410403.

7. Kuban DA, Tucker SL, Dong L, Starkschall G, Huang EH, Cheung MR, et al. Long-term results of the M. D. Anderson randomized dose-escalation trial for prostate cancer. *Int J Radiat Oncol Biol Phys*. 2008;**70**(1):67-74. doi: 10.1016/j.ijrobp.2007.06.054. PubMed PMID: 17765406.
8. Zhang SX, Gao J, Buchholz TA, Wang Z, Salehpour MR, Drezek RA, et al. Quantifying tumor-selective radiation dose enhancements using gold nanoparticles: a monte carlo simulation study. *Biomed Microdevices*. 2009;**11**(4):925-33. doi: 10.1007/s10544-009-9309-5. PubMed PMID: 19381816.
9. Zhang XD, Guo ML, Wu HY, Sun YM, Ding YQ, Feng X, et al. Irradiation stability and cytotoxicity of gold nanoparticles for radiotherapy. *Int J Nanomedicine*. 2009;**4**:165-73. doi: 10.2147/IJN.S6723. PubMed PMID: 19774115; PubMed PMCID: PMC2747351.
10. Cho SH, Jones BL, Krishnan S. The dosimetric feasibility of gold nanoparticle-aided radiation therapy (GNRT) via brachytherapy using low-energy gamma-/x-ray sources. *Phys Med Biol*. 2009;**54**(16):4889-905. doi: 10.1088/0031-9155/54/16/004. PubMed PMID: 19636084; PubMed PMCID: PMC3064075.
11. Cho SH. Estimation of tumour dose enhancement due to gold nanoparticles during typical radiation treatments: a preliminary Monte Carlo study. *Phys Med Biol*. 2005;**50**(15):N163-73. doi: 10.1088/0031-9155/50/15/N01. PubMed PMID: 16030374.
12. Chithrani BD, Ghazani AA, Chan WC. Determining the size and shape dependence of gold nanoparticle uptake into mammalian cells. *Nano Lett*. 2006;**6**(4):662-8. doi: 10.1021/nl052396o. PubMed PMID: 16608261.
13. Kong T, Zeng J, Wang X, Yang X, Yang J, McQuarrie S, et al. Enhancement of radiation cytotoxicity in breast-cancer cells by localized attachment of gold nanoparticles. *Small*. 2008;**4**(9):1537-43. doi: 10.1002/smll.200700794. PubMed PMID: 18712753.
14. McMahon SJ, Mendenhall MH, Jain S, Currell F. Radiotherapy in the presence of contrast agents: a general figure of merit and its application to gold nanoparticles. *Phys Med Biol*. 2008;**53**(20):5635-51. doi: 10.1088/0031-9155/53/20/00. PubMed PMID: 18812647.
15. Khan FM. The physics of radiation therapy. 4th ed. Philadelphia: Lippincott Williams & Wilkins, 2010.
16. Gasiorowicz S. Quantum Physics.3rdedition. New York: John Wiley & Sons, Inc., 2005.
17. Roeske JC, Nunez L, Hoggarth M, Labay E, Weichselbaum RR. Characterization of the theorectical radiation dose enhancement from nanoparticles. *Technol Cancer Res Treat*. 2007;**6**(5):395-401. PubMed PMID: 17877427.
18. Ibbott GS. Clinical applications of gel dosimeteres. *J Phys Conf Ser*. 2006;**56**(108):108-131. doi: 10.1088/1742-6596/56/1/010.
19. McJury M, Oldham M, Cosgrove VP, Murphy PS, Doran S, Leach MO, et al. Radiation dosimetry using polymer gels: methods and applications. *Br J Radiol*. 2000;**73**(873):919-29. doi: 10.1259/bjr.73.873.11064643. PubMed PMID: 11064643.
20. Marques T, Schwarcke M, Garrido C, Zucolot V, Baffa O, Nicolucci P. Gel dosimetry analysis of gold nanoparticle application in kilovoltage radiation therapy. *J Phys Conf Ser.* 2010;**250**(1):012084. doi:10.1088/1742-6596/250/1/012084.
21. Rahman WN, Wong CJ, Ackerly T, Yagi N, Geso M. Polymer gels impregnated with gold nanoparticles implemented for measurements of radiation dose enhancement in synchrotron and conventional radiotherapy type beams. *Australas Phys Eng Sci Med*. 2012;**35**(3):301-9. doi: 10.1007/s13246-012-0157-x. PubMed PMID: 22892958.
22. Sobczak-Kupiec A, Malina D, Zimowska M, Wzorek Z. Characterization of gold nanoparticles for various medical application. *Digest Journal Nanomaterial and Biostructures*. 2011;**6**(2):803-8. doi: 10.1117/12.907111.
23. Fernandes JP, Pastorello BF, de Araujo DB, Baffa O. Formaldehyde increases MAGIC gel dosimeter melting point and sensitivity. *Phys Med Biol*. 2008;**53**(4):N53-8. doi: 10.1088/0031-9155/53/4/N04. PubMed PMID: 18263941

24. Rivard MJ, Coursey BM, DeWerd LA, Hanson WF, Huq MS, Ibbott GS, et al. Update of AAPM Task Group No. 43 Report: A revised AAPM protocol for brachytherapy dose calculations. *Med phys*. 2004;**31**(3):633-74. doi: 10.1118/1.1646040. PubMed PMID: 15070264.

25. Khoshgard K, Hashemi B, Arbabi A, Rasaee MJ, Soleimani M. Radiosensitization effect of folate-conjugated gold nanoparticles on HeLa cancer cells under orthovoltage superficial radiotherapy techniques. *Phys Med Biol*. 2014;**59**(9):2249-63. doi: 10.1088/0031-9155/59/9/2249. PubMed PMID: 24733041.